Hindawi
Mathematical Problems in Engineering
Volume 2022, Article ID 7548608, 11 pages
https://doi.org/10.1155/2022/7548608

Research Article

A Semi-Markov Process Model for Performance Evaluation of DSRC Vehicular Safety Communication

Lin Hu,[1] **Xingyue Liu**,[1,2] **and Kun Zhou**[2]

[1]*Department of Electronic Information and Electrical Engineering, Chengdu University, Chengluo Road, Chengdu 610106, China*
[2]*Key Laboratory of Intelligent Manufacturing Quality Big Data Tracing and Analysis of Zhejiang Province, China Jiliang University, Hangzhou 310018, China*

Correspondence should be addressed to Lin Hu; hulin@cdu.edu.cn

Received 25 August 2022; Accepted 11 October 2022; Published 22 October 2022

Academic Editor: Zhihong Yao

In this study, a new semi-Markov process (SMP)-based model is devised to evaluate the IEEE 802.11p enhanced distributed channel access (EDCA) broadcast performance for vehicular safety communication. Differing from the existing SMP analytical models, the proposed model takes the virtual collision among various prioritized access categories (ACs) inside each vehicle into consideration. Moreover, in contrast to the Markov chain-based models, our model is simpler but with approximate accuracy. Concretely, we first capture the behavior of each AC's backoff entity using SMP. Then, the parameters of interest in the vehicular ad hoc network (VANET) such as packet transmission probability, conditional collision probability, and saturation throughput are derived. Finally, via MATLAB simulations, we demonstrate that the newly developed model achieves comparable accuracy in calculating these output parameters while its complexity and computation time is around one-tenth of that of the Markov chain-based models. Therefore, the proposed model is more suitable for real-time performance analysis of IEEE 802.11p EDCA safety communication in a freeway scenario.

1. Introduction

Thanks to the advanced wireless communication technologies, the intelligent transportation system (ITS) is projected to provide safe, effective, and high-quality future transportation systems [1]. The vehicular ad hoc network (VANET) had been viewed as an effective and efficient approach to satisfy ITS's claims by offering miscellaneous safety and nonsafety applications. Dedicated short-range communication (DSRC) is the most prospective candidate to implement the new generation of a worldwide VANET. It works at a 5.9 GHz band ranging from 5.850–5.925 GHz, which is specified by the US Federal Communication Commission (FCC) [2]. The assigned 75 MHz band contains a 10 MHz control channel (CCH) and six 10 MHz service channels (SCHs) where the CCH is exclusive for common safety communications and the SCHs are for other nonsafety applications. The physical (PHY) layer and the medium access control (MAC) sublayer of DSRC utilize the IEEE 802.11p wireless access vehicular environment (WAVE) standard, which inherits from the IEEE 802.11 standard [3]. To be specific, the physical (PHY) layer of DSRC adopts orthogonal frequency-division multiplexing (OFDM) modulation scheme that is the same as the IEEE 802.11a standard but supports transmission rates from 3 to 27 Mb/s since it generally adopts half of the bandwidth as the IEEE 802.11a protocol, the MAC sublayer of which adopts enhanced distributed channel access (EDCA) to guarantee the quality-of-service (QoS) [4].

Due to the highly dynamic topology and strict requirements in VANET, safety-related messages tend to be broadcast on CCH in a one-hop manner [5]. In a vehicle, the EDCA mechanism classifies safety-related messages from various applications into four following access categories (ACs) with corresponding priorities based on their criticalities to vehicles' safety: (1) AC[0], who has the highest priority, conveys urgent information from a wayside unit such as traffic accidents and appalling road condition and from abnormal vehicles in front including brake failure and over speeding; (2) AC [1], who has higher precedence than AC [2] but lower precedence than AC[0], conveys the position and speed information advertised by the vehicle; (3) AC [2], who has higher precedence than AC [3] but lower precedence than AC [1], conveys the information released by vehicles asking for help when they are risk-free to other vehicles such as overheating or running out of gas; (4) AC [3], who has the lowest priority, communicates information aimed at setting up new nonsafety-related conversations through the SCHs. It is worth noting that these four ACs are all broadcast via the CCH.

This study concerns the performance evaluation of safety-related messages broadcast on the CCH adopting IEEE 802.11p EDCA in a VANET environment. The main contributions of this study can be summarized as follows:

(1) We establish a new semi-Markov process (SMP)-based model to evaluate the IEEE 802.11p EDCA broadcast performance for vehicular safety communication under saturated conditions.
(2) Different from the existing SMP analytical models, we calculate the key performance indicators such as packet transmission probability, conditional collision probability, and saturation throughput by taking the virtual collision among four prioritized ACs inside each vehicle, namely, arbitration interframe space (AIFS) differentiation, the retry limit, the minimum, and maximum contention window (CW) into consideration.
(3) Compared with the Markov chain-based models, our model is simpler but with approximate accuracy.

The rest of this study is well organized as follows: we first introduce a VANET model and provide the necessary assumptions for a typical freeway scenario. Then, the analytical model of single-hop broadcast based on the IEEE 802.11p EDCA mechanism to assess the performance from the view of a certain reference vehicle is established. In the simulations, we validate the accuracy of the built model, and its complexity and computation time are calculated using MATLAB simulator and then compared with the existing Markov chain-based models. Finally, the conclusion of this study is carried out.

2. State of the Art

Bianchi [6] initially proposed a 2-D Markov-chain model for performance evaluation of the IEEE 802.11 distributed coordination function (DCF) protocol. The state space $[S]$ of the model in [6] can be easily computed by

$$[S] = \sum_{i=0}^{m} 2^i \left(CW_{\min} + 1\right), \tag{1}$$

where i denotes the backoff stage of the binary exponential backoff mechanism, $CWmin$ represents the minimum CW, and m stands for the maximum backoff stage. The state space $[S]$ is as follows:

$$[S] = \sum_{i=0}^{6} 2^i (15 + 1) = 16 \times \left(2^7 - 1\right) = 2032, \tag{2}$$

for frequency-hopping spread spectrum (FHSS) physical layer specifications.

Many of the previous research studies on performance analysis of VANET broadcast are grounded on Bianchi's model, such as [7–10]. Also, some works extended the 2-D model into a 3-D model. For example, in the work of [11], Hwuang and Chang developed a 3-D Markov chain-based model to assess the performance of IEEE 802.11e EDCA protocol. Moreover, other analytical models combining two Markov chains were established for the IEEE 802.11p EDCA. In [12], a 1-D Markov model was used to model the backoff instance of highest precedence, AC[0], and a 2-D Markov model for lower precedence, AC [1]-AC [3]. Authors in [13–15] built a 2-D Markov model for the backoff procedure of an AC queue and a 1-D Markov model for the contention period of an AC queue. In addition to the above works, Gallardo et al. [16] proposed different models for each of the access categories AC [1] through AC [3], and Zhao et al. [17] employed a scalable analytical model to capture the IEEE 802.11p EDCA performance. Intuitively, the state space $[S]$ of Bianchi's model is with the order of $O(2^m)$ which is very large, let alone the theoretical models mentioned above for the more sophisticated IEEE 802.11p EDCA protocol.

For simplicity and reduced complexity, SMP-based models for performance assessment of IEEE 802.11 DCF protocol have been devised in [18, 19]. The proposed models had a lessened number of states with the order of $O(m)$ compared to that of Bianchi's model with the order of $O(2^m)$. The SMP model approach has also been exploited in the performance assessment of IEEE 802.11p EDCA. Yin et al. [20] introduced an SMP model for MAC level performance assessment of one type of safety service in a single channel. The authors in [21] extended the model to multichannel services and the model was extended to MAC and application-level performance evaluation in [22]. Reference [23] presented an SMP model for basic safety message broadcast performance analysis and various QoS metrics were defined and evaluated. However, all these works only consider the performance evaluation of a certain type of AC. The performance of multiple types of safety messages was analyzed in [24] using an SMP model. However, their work did not consider the virtual collisions and assumed that all ACs in a node were independent from each other which is not reasonable. A detailed survey and analysis of the most related models is shown in this study and generalized in Table 1.

Motivated by the above-mentioned observations, we design an SMP-based analytical model for the IEEE 802.11p EDCA performance assessment for vehicular safety communication and derive the key performance indicators such as conditional collision probability, packet transmission probability, and saturation throughput. As far as we know, this is the first SMP-based analytical model designed for the performance of multiple types of safety message broadcast taking the virtual collisions into consideration, which can not only accurately calculate these output parameters but

Table 1: Comparison of analytical models.

Reference	Approach	Mode	MAC type	AD	Number of AC	VC	Throughput
[6–17]	Markov chain-based	U/B	DCF/EDCA	—	1/2/3/4	×/√	√
[18, 19]	SMP based	U	DCF	—	—	—	√
[20–23]	SMP based	B	EDCA	×	1	×	×
[24]	SMP based	B	EDCA	√	4	×	×
Our model	SMP based	B	EDCA	√	4	√	√

Note: U: unicast, B: broadcast, AD: AIFS differentiation, VC: virtual collision, and ×: not considered.

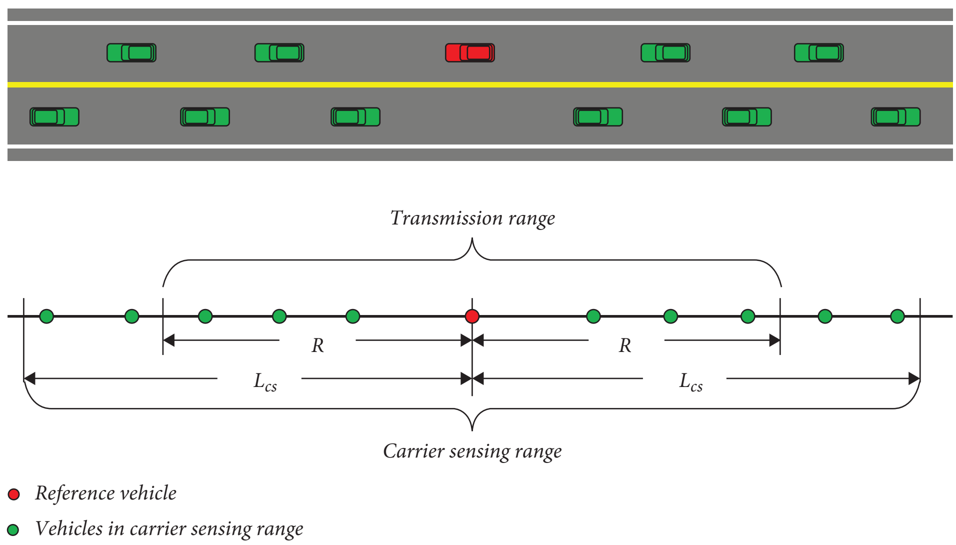

Figure 1: The diagram of the 1-D VANET model.

also achieve results with less complexity and computation time compared with the existing Markov chain-based models.

3. System Model and Assumptions

We first introduce the VANET model in the freeway scenario in this section. To facilitate modeling, we then enumerate some essential and reasonable assumptions.

3.1. System Model. Imagine that several vehicles run on a bidirectional freeway and each direction has one lane. Since the maximum transmission range defined in the IEEE 802.11p standard is up to 1 km and the width of two lanes is around 10 m, which can be neglected, we can then simplify this typical freeway scenario into a 1-D VANET model, which is illustrated in Figure 1.

In this model, one node stands for one vehicle. The transmission range defined as the maximum distance between a pair of transceivers that can successfully contact each other is denoted by R. It depends on the transmission power and wireless channel condition. Also, we define the carrier sensing range as the maximum distance that a node can detect a signal and denote it as L_{cs}, which is a crucial parameter in the carrier sense multiple access/collision avoidance (CSMA/CA) technique.

3.2. Assumptions. We suppose the following scenarios for IEEE 802.11p VANET broadcasting in a freeway scenario:

(1) Vehicles are placed exponentially on a 1-D freeway whose distribution satisfies Poisson point process with parameter β (in vehicles per meter); then, the probability of finding i vehicles existing in length l is obtained by

$$P(i,l) = \frac{(\beta l)^i}{i!} e^{-\beta l}. \quad (3)$$

(2) As shown in Figure 1, with the constraint $R \le L_{cs}$, we can readily figure out the mean number of vehicles in the transmission range and the carrier sensing range, respectively, as follows:

$$\begin{cases} N_{tr} = 2\beta R, \\ N_{cs} = 2\beta L_{cs}. \end{cases} \quad (4)$$

(3) Safety-related messages are usually very short, so each of them can be encapsulated in a single packet [4]. Also, we assume that all ACs have the same mean packet size P_D.

(4) The IEEE 802.11p EDCA protocol provides each AC with a MAC queue entity to occupy the medium and each entity always has a packet available for transmission, i.e., saturation condition.

TABLE 2: Access parameter for IEEE 802.11p EDCA.

AC	CW_{min}	CW_{max}	AIFSN	TXOP limit
3	aCW_{min}	aCW_{max}	9	0
2	aCW_{min}	aCW_{max}	6	0
1	$(aCW_{min}+1)/2-1$	aCW_{min}	3	0
0	$(aCW_{min}+1)/4-1$	$(aCW_{min}+1)/2-1$	2	0

(5) In this study, we only emphasize the influences of internal and external collisions on network performance. Hence, the impact of an error-prone channel is neglected. Such consideration can be readily extended from existing results such as [24, 25].

4. Analytical Model

In this section, we expound on our analytical model for the IEEE 802.11p EDCA safety messages broadcast.

4.1. Differentiation Parameters in EDCA. The IEEE 802.11p EDCA distinguishes ACs by identifying channel access parameters, which include the CW, the AIFS, and the transmission opportunity (TXOP). Table 2 lists the specific access parameter of IEEE 802.11p EDCA, where AC [0] corresponds to the highest priority and AC [3] corresponds to the lowest priority.

(1) *CW*: let $W_{i,j}$ be the maximum CW size of AC[i] ($i=0, 1, 2, 3$) at the jth backoff stage after j times failed transmission attempts; hence, $W_{i,0}=CW_{i,min}+1$. Denote M_i as the maximum times the CW of AC[i] can be doubled; thus, $M_i = \log_2((CW_{i,\max}+1)/CW_{i,\min}+1)$. Therefore, $W_{i,j}$ can be computed by

$$W_{i,j} = \begin{cases} 2^j W_{i,0}, & j \le M_i, \\ 2^{M_i} W_{i,0}, & M_i < j \le L_i, \end{cases} \tag{5}$$

where L_i is the retry limit for AC[i] packets. For convenience, we assume that all L_i equals L in this study.

(2) *AIFS*: to support priority-based QoS, EDCA defines a different defer time called AIFS for ACs when the channel is detected free. The duration of AIFS is determined by the AIFS number (AIFSN) according to the following:

$$\text{AIFS}[i] = \text{SIFS} + \text{AIFSN}[i] \times \sigma, \tag{6}$$

where σ is the slotted time, SIFS represents the short interframe space, and $\text{AIFSN}[i] \ge 2$. Define A_i as the AIFS differentiation, which is given by

$$A_i = \text{AIFSN}[i] - \text{AIFSN}[0]. \tag{7}$$

(3) *TXOP*: the TXOP limit permits an AC entity to consecutively transmit several packets without channel contentions. However, the TXOP limit still has not been fixed by the IEEE 802.11p standard up to now. In this study, we assume it equals zero, which indicates an AC entity has to compete for the channel access opportunity every time it accomplishes a packet transmission.

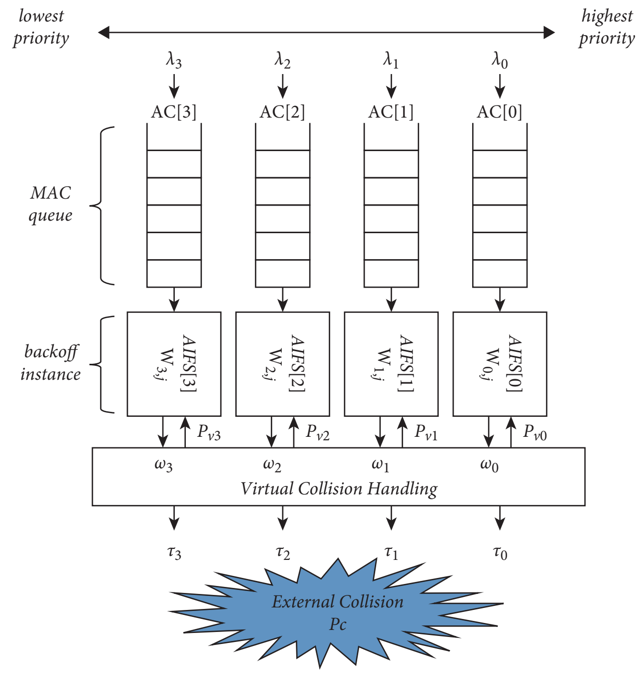

FIGURE 2: The diagram of IEEE 802.11p EDCA backoff procedure.

4.2. IEEE 802.11p EDCA Broadcast Mechanism. As shown in Figure 2, new different prioritized packets arrive at the MAC layer from higher layers and then are assigned to corresponding queues. Without considering the virtual collisions, the backoff instances in a station can be regarded as being independent from every single other. For each AC, it transmits if the channel is sensed vacant for an AIFS. Otherwise, the AC will keep monitoring the channel until the idle duration up to the AIFS. At present, a backoff procedure is triggered and a random interval is generated according to the AC's CW value. The backoff counter starts to decrease only if the channel stays vacant for an AIFS. When the backoff counter reaches zero, it will be transmitted. Since safety messages tend to be broadcast, there is no ACK mechanism and the packet will be discarded regardless of the successful or failed transmission.

When taking the virtual collision into account, different backoff instances in a node cannot occupy the channel all alone. Figure 2 presents a summarization of a station with virtual collision handling. If more than two backoff instances of a node are attempting to use the channel at the same time, a virtual collision happens. On this occasion, the packet that has the highest priority should be transmitted, and the packets with lower priorities enter another backoff stage with doubled CWs directly. If the failed retransmission count reaches the retry limit, it will be dropped.

As demonstrated in Figure 2, we denote the internal transmission probability that the backoff instance of AC[i] tries to transmit a packet in a timeslot observed by other ACs in the same node and the internal collision probability of AC [i] as ϖ_i and p_{vi}, respectively. Accordingly, it has the following:

$$\begin{cases} p_{v0} = 0, \\ p_{v1} = \varpi_0, \\ p_{v2} = 1 - (1 - \varpi_0)(1 - \varpi_1), \\ p_{v3} = 1 - (1 - \varpi_0)(1 - \varpi_1)(1 - \varpi_2). \end{cases} \tag{8}$$

The external transmission probability τ_i observed by other nodes outside of the node is computed by the following:

$$\begin{cases} \tau_0 = \varpi_0 (1 - p_{v0}) = \varpi_0, \\ \tau_1 = \varpi_1 (1 - p_{v1}) = \varpi_1 (1 - \varpi_0), \\ \tau_2 = \varpi_2 (1 - p_{v2}) = \varpi_2 (1 - \varpi_0)(1 - \varpi_1), \\ \tau_3 = \varpi_3 (1 - p_{v3}) = \varpi_3 (1 - \varpi_0)(1 - \varpi_1)(1 - \varpi_2). \end{cases} \tag{9}$$

Hence, the total transmission probability τ for a node can be written as follows:

$$\tau = \tau_0 + \tau_1 + \tau_2 + \tau_3. \tag{10}$$

The external collision probability p_c is calculated by the following:

$$\begin{aligned} p_c &= 1 - \sum_{k=0}^{\infty} (1 - \tau)^k \frac{(N_{cs} - 1)^k}{k!} e^{-(N_{cs} - 1)} \\ &= 1 - e^{-(N_{cs} - 1)\tau}. \end{aligned} \tag{11}$$

We can observe from equation (11) that p_c is obtained by 1 minus the successful transmission probability of the reference node. The following condition should be satisfied to ensure a successful transmission: when the reference node is transmitting, no nodes in its carrier sensing range transmit simultaneously. The average packet transmission time is given as follows:

$$T_{tr} = \frac{PHY_H}{R_b} + \frac{MAC_H + E[P]}{R_d} + \delta, \tag{12}$$

where $E[P]$ represents the average length of the data packet from the upper layer, PHY_H and MAC_H stand for the lengths of packet header from physical and MAC layer separately, R_b and R_d, respectively, denote the basic rate and data rate and δ is the propagation delay.

4.3. SMP Model. In this part, the backoff procedure of AC[i] is simulated using an SMP approach. In the SMP model, an average state sojourn time, the duration that a node stays at the current state before making a state change from the present state, is incorporated. The subsequent state of the node in the SMP model hinges on the present state and its state sojourn time. The sample paths for the SMP model are timed sequences of the state transitions. If the process is seen at the instances of state transitions, the sample paths are the same as those of a Markov chain. Such a process is called the embedded Markov chain, which does not contain self-loops [26].

In the following part, we first construct a $(L_i + 1)$-state Markov chain to figure out the backoff stages of AC[i]. Given that the backoff interval involved in different backoff stages of AC[i] are not identical, this discrete-time Markov chain with a unit state sojourn time for all the states cannot exactly capture the behavior of the backoff procedure of AC[i], which then brings about the introduction of an embedded Markov chain allowing different state sojourn times for different states. However, this embedded Markov chain does not include self-loops (switching from the state j to itself). Thus, we subsequently model the backoff procedure of AC[i] with the SMP model allowing self-loops and different state sojourn times for different backoff stages. Ultimately, we calculate the parameters of interest grounded on the proposed SMP model.

The $(L_i + 1)$-state Markov chain in Figure 3 stands for the backoff procedure of AC[i]. The backoff instance of AC[i] with packets to send is in state 0. If the AC[i] escapes from virtual collision, its backoff instance loops back to state 0 and starts the next packet transmission. For virtual collision, the backoff instance of AC[i] in state j, $j \in [0, L_i - 1]$, proceeds retransmission and goes into state $j + 1$. For the backoff instance of AC[i] in state L_i, it will always go into state 0 whether the packet is free from virtual collision or not. But it is different that for the case where no virtual collision happens in state L_i, the backoff instance of AC[i] initiates a new packet transmission, while for the case where AC[i] suffers from virtual collision, it will drop the transmitting packet directly and then begin a new packet transmission. The changing from state j to state $j + 1$ indicates that the AC [i] packet transmission encounters the virtual collision and the transition from any state j, $j \in [0, L_i - 1]$, to state 0 indicates the AC[i] escapes from the virtual collision. The loopback is only possible for the state 0.

The state transitions of the $(L_i + 1)$-state Markov chain can be described by the one-step state transition probability matrix P^i given by the following:

$$P^i = \begin{bmatrix} 1 - p_{vi} & p_{vi} & 0 & 0 & \cdots & 0 & 0 \\ 1 - p_{vi} & 0 & p_{vi} & 0 & \cdots & 0 & 0 \\ 1 - p_{vi} & 0 & 0 & p_{vi} & \cdots & 0 & 0 \\ 1 - p_{vi} & 0 & 0 & 0 & \cdots & 0 & 0 \\ \bullet & \bullet & \bullet & \bullet & \bullet & \bullet & \bullet \\ 1 - p_{vi} & 0 & 0 & 0 & \cdots & p_{vi} & 0 \\ 1 - p_{vi} & 0 & 0 & 0 & \cdots & 0 & p_{vi} \\ 1 & 0 & 0 & 0 & \cdots & 0 & 0 \end{bmatrix}, \tag{13}$$

where $p^i_{j,k}$, $0 \leq j$, $k \leq L_i$, is the probability of transition from state j to state k and $p^i_{j-1,j}$, $1 \leq j \leq L_i$, is equal to the internal collision probability p_{vi}.

Then, we transform the above Markov chain into an embedded Markov chain (with $p^i_{j,j} = 0, \forall j$), as illustrated in Figure 4.

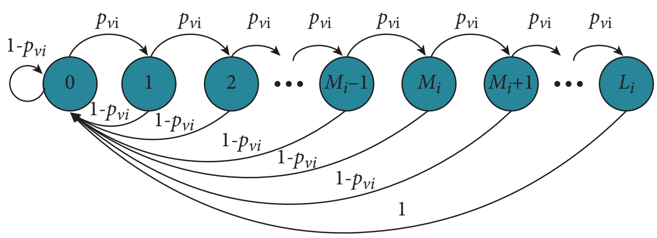

FIGURE 3: The $(L_i + 1)$-state Markov chain of AC[i].

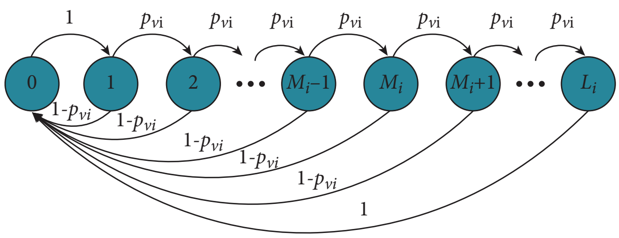

FIGURE 4: The $(L_i + 1)$-state embedded Markov chain of AC[i].

The element $p^{e,i}_{j,k}$ of the state transition probability matrix $P^{e,i}$ of the embedded Markov chain is given by the following:

$$p^{e,i}_{j,k} = \begin{cases} 0, & \text{for}\, j = k, \\ \dfrac{p^{i}_{j,k}}{1 - p^{i}_{j,j}}, & \text{for}\, j \neq k, \end{cases} \tag{14}$$

which results in the following:

$$P^{e,i} = \begin{bmatrix} 0 & 1 & 0 & 0 & \cdots & 0 & 0 \\ 1 - p_{vi} & 0 & p_{vi} & 0 & \cdots & 0 & 0 \\ 1 - p_{vi} & 0 & 0 & p_{vi} & \cdots & 0 & 0 \\ 1 - p_{vi} & 0 & 0 & 0 & \cdots & 0 & 0 \\ \bullet & \bullet & \bullet & \bullet & \bullet & \bullet & \bullet \\ 1 - p_{vi} & 0 & 0 & 0 & \cdots & p_{vi} & 0 \\ 1 - p_{vi} & 0 & 0 & 0 & \cdots & 0 & p_{vi} \\ 1 & 0 & 0 & 0 & \cdots & 0 & 0 \end{bmatrix}. \tag{15}$$

The stationary probability $\pi^{e,i}_j$ of the state j of the embedded Markov chain is derived by the following:

$$\pi^{e,i}_j = \sum_{k \neq j} \pi^{e,i}_k p^{e,i}_{k,j}, \quad \forall j \in [0, L_i]. \tag{16}$$

Combining these simultaneous equations with $\sum_{j=0}^{L_i} \pi^{e,i}_j = 1$, we acquire the stationary probabilities of the embedded Markov chain by the following:

$$\pi^{e,i}_0 = \pi^{e,i}_1 = \frac{1 - p_{vi}}{\left(2 - p_{vi} - p^{L_i}_{vi}\right)},$$
$$\pi^{e,i}_j = \frac{(1 - p_{vi}) p^{j-1}_{vi}}{\left(2 - p_{vi} - p^{L_i}_{vi}\right)}, \quad \forall j \in [2, L_i]. \tag{17}$$

which constitute the stationary probability vector $\pi^{e,i}$ marked as $[\pi^{e,i}_0, \pi^{e,i}_1, \pi^{e,i}_2, \ldots, \pi^{e,i}_{L_i}]$.

Based on [26], the stationary probabilities vector $\pi^{s,i}$ of the SMP model is denoted as $[\pi^{s,i}_0, \pi^{s,i}_1, \pi^{s,i}_2, \ldots, \pi^{s,i}_{L_i}]$, and

$$\pi^{s,i}_j = \frac{\pi^{e,i}_j \times E\left[H^i_j\right]}{\sum_{k=0}^{L_i} \left\{\pi^{e,i}_k \times E\left[H^i_k\right]\right\}}, \quad 0 \leq j \leq L_i, \tag{18}$$

where H^i_j represents the sojourn time of state j. The backoff interval of the backoff stage j is modeled with the state sojourn time, which is a random variable uniformly chosen within the range $[0, W_{i,j}]$, for $0 \leq j \leq L_i$.

Since high priority ACs' AIFSs will affect low priority ones, the probability for each AC's backoff counter to decrease one may not be identical. Let p_{bi} be the backoff blocking probability. For a given backoff instance of AC[i] in a vehicle, p_{bi} equals the possibility that the vehicle senses other vehicles using the channel or other ACs in the same vehicle are attempting transmissions. Due to the bigger AIFSNs, the lower priority ACs are deferred for a longer time than higher priority ones, which is shown in Figure 5. Hence, p_{bi} is computed by the following:

$$p_{bi} = 1 - \left[\sum_{k=0}^{\infty} (1 - \tau)^k \frac{(N_{cs} - 1)^k}{k!} e^{-(N_{cs} - 1)} \prod_{\substack{j=0 \\ j \neq i}}^{3} \left(1 - \varpi_j\right)\right]^{A_i + 1}, \tag{19}$$

then, the average slot time $\overline{\sigma_i}$ for each AC in a vehicle is obtained by the following:

$$\overline{\sigma_i} = p_{bi} T_{tr} + (1 - p_{bi}) \sigma, \tag{20}$$

and the normalized slot time for each AC in a vehicle is written as follows:

$$\left|\overline{\sigma_i}\right| = \frac{\overline{\sigma_i}}{\sigma}. \tag{21}$$

Therefore, the expected value of state sojourn time $E[H^i_j]$ for state j of the semi-Markov process of AC[i] is given by the following:

$$E\left[H^i_j\right] = \frac{W_{i,j}}{2} \left|\overline{\sigma_i}\right|, \quad 0 \leq j \leq L_i. \tag{22}$$

For the given backoff instance of AC[i], it will visit state 0 successively after successfully escaping from the virtual collision in backoff stage j, $0 \leq j \leq L_i$, and after a packet drop

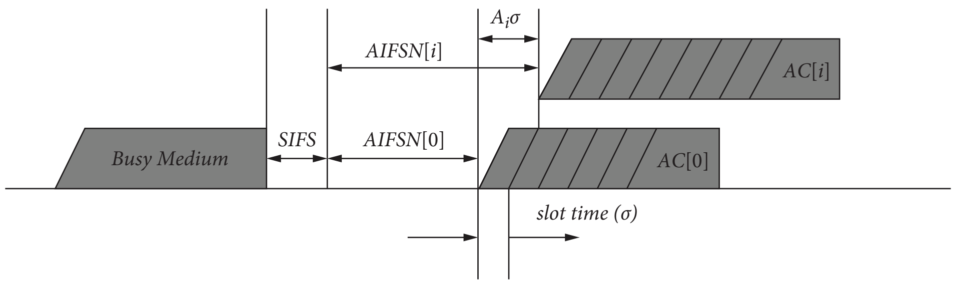

Figure 5: Illustration of the impact of different AIFSNs on backoff blocking probability.

in backoff stage L_i. Hence, the excepted number of consecutive visits to state 0 is $1/(1-(1-p_{vi}))$, and the expected value of state sojourn time for state 0 is as follows:

$$E\left[H_0^i\right] = \frac{W_{i,0}}{2}\left|\overline{\sigma_i}\right| \times \frac{1}{p_{vi}} = \frac{W_{i,0}}{2p_{vi}}\left|\overline{\sigma_i}\right|. \tag{23}$$

Using equation (18) and $\sum_{j=0}^{L_i}\pi_j^{s,i}=1$, the stationary probabilities of the SMP of AC[i] are given by the following:

$$\begin{aligned}\pi_0^{s,i} &= \frac{1}{2B_i p_{vi}},\\ \pi_1^{s,i} &= \frac{1}{B_i},\\ \pi_j^{s,i} &= \begin{cases}\dfrac{(2p_{vi})^{j-1}}{B_i}, & 2\le j\le M_i,\\[2ex] \dfrac{2^{M_i-1}p_{vi}^{j-1}}{B_i}, & M_i<j\le L_i,\end{cases}\end{aligned} \tag{24}$$

where

$$B_i = \frac{1-(2p_{vi})^{M_i+1}}{2p_{vi}(1-2p_{vi})} + 2^{M_i-1}\frac{p_{vi}^{M_i}-p_{vi}^{L_i}}{1-p_{vi}}. \tag{25}$$

The stationary probability $\pi_j^{s,i}$ of the SMP represents the fraction of time spent by AC[i] in backoff stage j.

In the following part, we exploit the stationary probability distribution of the SMP model and the state sojourn times to derive the packet transmission probability τ, conditional collision probability (i.e., external collision probability), and saturated network throughput. The internal transmission probability ϖ_i is computed as follows:if the backoff instance of AC[i] is in state j, it will transmit once after an expected time interval $E[H_j]$, for $1\le j\le L_i$. For state 0, AC[i] transmits once after an expected time interval of $E[H_0]/(1/p_{vi})$. Hence, ϖ_i can be expressed as follows:

$$\begin{aligned}\varpi_i &= \frac{\pi_0^{s,i}(1/p_{vi})}{E[H_0]} + \frac{\pi_1^{s,i}}{E[H_1]} + \cdots + \frac{\pi_{L_i}^{s,i}}{E\left[H_{L_i}\right]}\\ &= \frac{1-p_{vi}^{L_i+1}}{B_i W_{i,0} p_{vi}(1-p_{vi})\left|\overline{\sigma_i}\right|}.\end{aligned} \tag{26}$$

So far, we have derived the internal transmission probability of AC[0]-AC [3] from the proposed SMP model and we can get the packet transmission probability τ by combining equations (8)–(10).

Let S_i be the saturation throughput for each AC in a station. Define P_{tr} as the possibility of at least one node in the transmission range transmitting in the considered slot time, $P_{s,i}$ as the probability that a transmission attempt of AC[i] is successful conditioned on the fact that at least one node transmitting in the considered slot time, and P_{fc} as the probability that a transmission attempt fails owing to a collision conditioned on the fact that at least one node transmitting in the considered slot time. Thus, we have the following:

$$\begin{cases} P_{tr} = 1-\sum\limits_{k=0}^{\infty}(1-\tau)^k\left(N_{tr}^k/k!\right)e^{-N_{tr}} = 1-e^{-N_{tr}\tau},\\[2ex] P_{s,i} = \dfrac{N_{tr}\times\tau_i\times\sum_{k=0}^{\infty}(1-\tau)^k\left((N_{cs}-1)^k/k!\right)e^{-(N_{cs}-1)}}{P_{tr}}, \quad i=0,1,2,3,\\[2ex] P_{fc} = \dfrac{1-\sum_{k=0}^{\infty}(1-\tau)^k\left(N_{tr}^k/k!\right)e^{-N_{tr}} - N_{tr}\times\tau\times\sum_{k=0}^{\infty}(1-\tau)^k\left((N_{cs}-1)^k/k!\right)e^{-(N_{cs}-1)}}{P_{tr}},\end{cases} \tag{27}$$

and S_i is derived by

Table 3: Parameters of highway scenario.

Parameters	Value
Highway length	1000 m
Density (β)	0.01~0.1 vehicles/m
Average vehicle distance	100 m~10 m
Total number of vehicles	10~100
Transmission range (R)	500 m
Carrier sensing range (L_{cs})	700 m

Table 4: Parameter settings of DSRC communication.

General parameters	Value
Data rate (R_d)	24 Mbps
Basic rate (R_b)	6 Mbps
Slot time (σ)	9 μsec
SIFS time	16 μsec
DIFS = SIFS + 2 × slot time	34 μsec
Propagation delay (δ)	1 μsec
Data payload length ($E(P)$)	200 octets
MAC sublayer overhead	28 octets
PHY layer overload	20 μsec
Retry limit L	7
$a\mathrm{CW}_{\min}$	63
$a\mathrm{CW}_{\max}$	1023

Table 5: Comparison of (τ, p_c, S) and (τ_B, p_B, S_B) for different vehicle densities, respectively.

N	(τ, p_c, S)	(τ_B, p_B, S_B)
2	(0.0740, 0.1248, 310.49 kB/s)	(0.0729, 0.1236, 312.56 kB/s)
3	(0.0625, 0.1813, 384.74 kB/s)	(0.0630, 0.1789, 382.98 kB/s)
5	(0.0511, 0.2640, 466.77 kB/s)	(0.0502, 0.2569, 467.76 kB/s)
10	(0.0397, 0.4030, 523.69 kB/s)	(0.0399, 0.4052, 519.71 kB/s)
20	(0.0319, 0.5772, 496.73 kB/s)	(0.0327, 0.5775, 493.79 kB/s)
30	(0.0287, 0.6915, 439.51 kB/s)	(0.0292, 0.6926, 441.52 kB/s)
40	(0.0270, 0.7729, 379.84 kB/s)	(0.0273, 0.7738, 381.56 kB/s)
50	(0.0259, 0.8326, 323.07 kB/s)	(0.0256, 0.8330, 321.10 kB/s)
60	(0.0252, 0.8768, 271.01 kB/s)	(0.0251, 0.8771, 271.06 kB/s)
70	(0.0248, 0.9095, 224.43 kB/s)	(0.0249, 0.9102, 221.48 kB/s)
80	(0.0245, 0.9338, 183.64 kB/s)	(0.0247, 0.9343, 186.68 kB/s)
90	(0.0242, 0.9517, 148.59 kB/s)	(0.0244, 0.9519, 145.63 kB/s)
100	(0.0241, 0.9648, 119.02 kB/s)	(0.0240, 0.9654, 116.07 kB/s)

$$S_i = \frac{P_{s,i} \times P_{tr} \times E[P]}{(1 - P_{tr})\sigma + \sum_{i=0}^{3} P_{tr} \times P_{s,i} \times t_{s,i} + P_{tr} \times P_{fc} \times t_{c,i}}, \quad (28)$$

where the expressions of $t_{s,i}$, and $t_{c,i}$ are given by

$$t_{s,i} = t_{c,i} = T_{tr} + \mathrm{AIFS}[i]. \quad (29)$$

5. Simulations

In this part, we conduct the experiments using MATLAB. First, the essential network parameters (τ, p_c, S) of VANET are calculated via the proposed SMP model where $S = \sum_{i=0}^{3} S_i$ is the aggregate throughput for all ACs, i.e., the overall throughput of each AC in a vehicle. Second, we evaluate the computation time for the proposed SMP model. To show our proposed model is less complex with high accuracy, we compare the experimental results from the proposed model with the results from the existing Markov chain-based models. In our study, we take Yao et al. model [12] as an example. The values of τ and p_c derived by Yao et al. model (by setting ρ_i and p_{ai} in the study equal to 1) are denoted as τ_B and p_B.

The parameters of the freeway scenario are listed in Table 3. The fixed-point iteration method is adopted to compute the conditional collision probability (p_c) and packet transmission probability (τ). These results were further used for calculating the saturated throughput of the network (though the formula of network throughput is not presented in Yao's paper, it can be derived in the same way as equation (28)). The input DSRC communication parameters are presented in Table 4. These calculations are carried out for

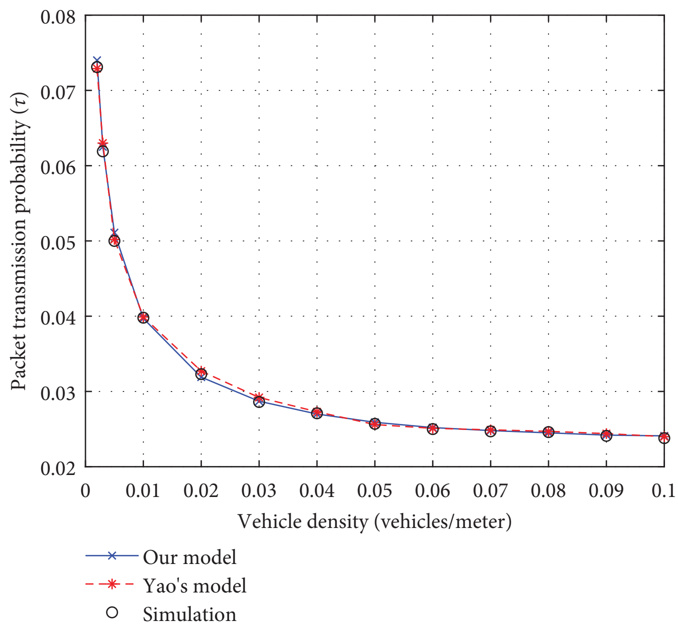

Figure 6: Packet transmission probabilities (τ) with different vehicle densities.

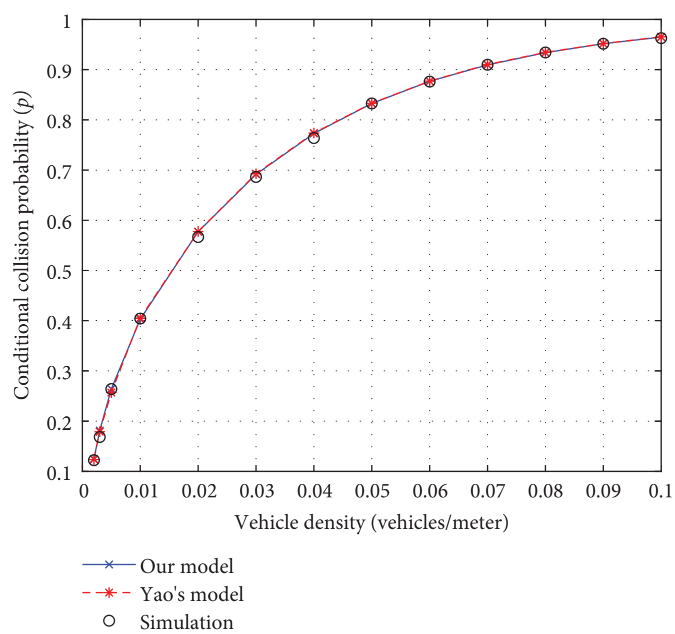

Figure 7: Conditional collision probabilities (p) with different vehicle densities.

different vehicle densities and the outputs obtained are compared with those from Yao et al. model (τ_B, $p_{B,}$ and S_B). The results obtained from these two models are listed in Table 5.

We can readily observe from Table 5 that the results of the proposed model are close to those of Yao's model with a maximum deviation of 0.1% for saturated throughput S. As β increases, the number of vehicles in the transmission range of the reference vehicle increases which results in p increasing and τ decreasing for both two models. Especially, while β increases, S steadily grows until it reaches its maximum value, then declines to zero as $\beta \longrightarrow \infty$. This trend is predictable referring to [6] and consistent with Yao's model. For better illustration, the comparisons between the theoretical results from Yao's model and the SMP model with the simulation results are presented in Figures 6–8. It is apparent that both the theoretical curves match the simulation result very well which validates the accuracy of our model.

For the computation time, it is acquired by exploiting the MATLAB commands *tic* and *toc*. Table 6 shows the MATLAB implementation times for the two models. It is visible that the computation times for both two models remain no change with different vehicle densities. More

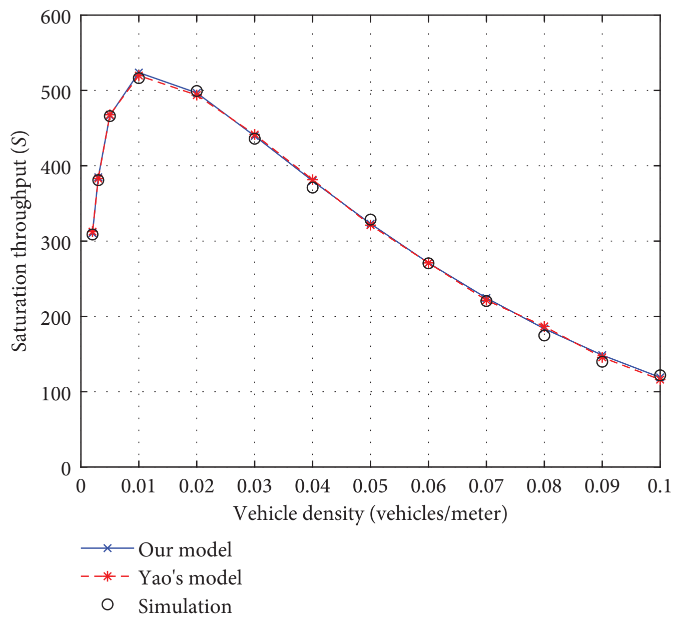

Figure 8: Aggregate throughputs of each AC (S) with different vehicle densities.

Table 6: Comparison of computational time for Yao's model (C_B) and our model (C).

N	C_B (in seconds)	C (in seconds)
2	8.058025	0.795876
3	8.608732	0.781768
5	8.202035	0.750957
10	8.175375	0.809911
20	8.136141	0.821079
30	7.988931	0.787711
40	8.563271	0.816115
50	8.361551	0.811665
60	8.063119	0.804857
70	7.873188	0.792516
80	8.589630	0.847394
90	8.132592	0.837210
100	7.624087	0.791316

importantly, as the state number of our model is with the order of $O(L)$ and the state number of Yao's model is with the order of $O(2^L)$, the proposed SMP model only uses nearly one-tenth of the time spent for computing the stationary probabilities of Yao's model, which proves the proposed SMP model is more effective than the existing Markov chain-based models.

6. Conclusions

In this study, we model the network performance of IEEE 802.11p EDCA for vehicular safety communication using the semi-Markov process. The newly constructed SMP model considers the impacts of virtual collisions and varying priorities among different ACs inside each EDCA station. Also, the output parameters including the packet transmission probability, conditional collision probability, and saturated throughput are calculated. Furthermore, the accuracy and conciseness of the proposed model are validated by experimental results.

Data Availability

The simulation parameter data used to support the findings of this study are included in the article.

Disclosure

A preprint has previously been published [27].

Conflicts of Interest

The authors declare that they have no conflicts of interest regarding the publication of this study.

Acknowledgments

This work was supported by the Open Research Project of Key Laboratory of Intelligent Manufacturing Quality Big Data Tracing and Analysis of Zhejiang Province, China Jiliang University (Grant No. ZNZZSZ-CJLU2022-06).

References

[1] G. Dimitrakopoulos and P. Demestichas, "Intelligent transportation systems," *IEEE Vehicular Technology Magazine*, vol. 5, no. 1, pp. 77–84, 2010.
[2] *Intelligent transportation services report and order*, U.S. Federal Communications Commission, Washington, DC, USA, 1998.
[3] L. Cao, "IEEE standard for information technology telecommunications and information exchange between systems local and metropolitan area networks specific requirements Part 11: wireless LAN medium access control (MAC) and

physical layer (PHY) specifications," *The Standard*, vol. 802, pp. 11–2016, 2016.

[4] J. B. Kenney, "Dedicated short-range communications (DSRC) standards in the United States," *Proceedings of the IEEE*, vol. 99, no. 7, pp. 1162–1182, 2011.

[5] X. Ma, J. Zhang, and T. Wu, "Reliability analysis of one-hop safety-critical broadcast services in vanets," *IEEE Transactions on Vehicular Technology*, vol. 60, no. 8, pp. 3933–3946, 2011.

[6] G. Bianchi, "Performance analysis of the IEEE 802.11 distributed coordination function," *IEEE Journal on Selected Areas in Communications*, vol. 18, no. 3, pp. 535–547, 2000.

[7] J. Peng, S. Li, Z. Dou, and S. Yang, "Optimization design and performance analysis of improved IEEE802.11p MAC mechanism based on high mobility of vehicle 802.11p MAC mechanism based on high mobility of vehicle," *Mathematical Problems in Engineering*, vol. 2022, Article ID 8974673, pp. 1–14, 2022.

[8] Y. Kim, M. Lee, and T.-J. Lee, "Coordinated multichannel MAC protocol for vehicular ad hoc networks," *IEEE Transactions on Vehicular Technology*, vol. 65, no. 8, pp. 6508–6517, 2016.

[9] L. Hu, H. Wang, and Y. Zhao, "Performance analysis of DSRC-based vehicular safety communication in imperfect channels," *IEEE Access*, vol. 8, Article ID 107399, 2020.

[10] X. Yang, Y. Mao, Q. Xu, and L. Wang, "Priority-based hybrid MAC protocol for VANET with UAV-enabled roadside units," *Wireless Communications and Mobile Computing*, vol. 2022, Article ID 8697248, 13 pages, 2022.

[11] I. Hwuang and H. Chang, "Performance assessment of IEEE 802.11e EDCF using three-dimension Markov chain model," *Applied Mathematical Sciences*, vol. 2, no. 3, pp. 139–151, 2008.

[12] Y. Yao, L. Rao, and X. Liu, "Performance and reliability analysis of IEEE 802.11p safety communication in a highway environment," *IEEE Transactions on Vehicular Technology*, vol. 62, no. 9, pp. 4198–4212, 2013.

[13] J. Zheng and Q. Wu, "Performance modeling and analysis of the IEEE 802.11p EDCA mechanism for VANET," *IEEE Transactions on Vehicular Technology*, vol. 65, no. 4, pp. 2673–2687, 2016.

[14] S. Cao and V. C. Lee, "An accurate and complete performance modeling of the IEEE 802.11p MAC sublayer for VANET," *Computer Communications*, vol. 149, pp. 107–120, 2020.

[15] F. Peng, K. Shafiee, and V. C. Leung, "Throughput modelling of differentiation schemes for IEEE 802.11e MAC protocol," in *Proceedings of the 2012 IEEE Vehicular Technology Conference*, pp. 1–5, Quebec City, Canada, April 2012.

[16] J. R. Gallardo, D. Makrakis, and H. T. Mouftah, "Mathematical analysis of EDCA's performance on the control channel of an IEEE 802.11 WAVE vehicular network," *EURASIP Journal on Wireless Communications and Networking*, vol. 2010, Article ID 489527, 31 pages, 2010.

[17] Q. Zhao, D. H. Tsang, and T. Sakurai, "A scalable and accurate nonsaturated IEEE 802.11e EDCA model for an arbitrary buffer size," *IEEE Transactions on Mobile Computing*, vol. 12, no. 12, pp. 2455–2469, 2013.

[18] M. K. Kadiyala, D. Shikha, R. Pendse, and N. Jaggi, "Semi-markov process based model for performance analysis of wireless LANs," in *Proceedings of the 2011 IEEE International Conference on Pervasive Computing and Communications Workshops*, pp. 613–618, Seattle, WA, USA, June 2011.

[19] W. Hao, G. Kang, and H. Kai, "An advanced semi-markov process model for performance analysis of wireless LANs," in *Proceedings of the 2012 IEEE Vehicular Technology Conference*, pp. 1–5, Quebec City, Canada, July 2012.

[20] X. Yin, X. Ma, and K. S. Trivedi, "An interacting stochastic models approach for the performance evaluation of DSRC vehicular safety communication," *IEEE Transactions on Computers*, vol. 62, no. 5, pp. 873–885, 2013.

[21] X. Yin, X. Ma, K. S. Trivedi, and A. Vinel, "Performance and reliability evaluation of BSM broadcasting in DSRC with multi-channel schemes," *IEEE Transactions on Computers*, vol. 63, no. 12, pp. 3101–3113, 2014.

[22] X. Yin, X. Ma, and K. S. Trivedi, "MAC and application level performance evaluation of beacon message dissemination in DSRC safety communication," *Performance Evaluation*, vol. 71, pp. 1–24, 2014.

[23] X. Ma and K. S. Trivedi, "SINR-based analysis of IEEE 802.11p/bd broadcast VANETs for safety services," *IEEE Transactions on Network and Service Management*, vol. 18, no. 3, pp. 2672–2686, 2021.

[24] L. Hu and Z. Dai, "Performance and reliability analysis of prioritized safety messages broadcasting in DSRC with hidden terminals," *IEEE Access*, vol. 8, Article ID 177112, 2020.

[25] G. J. Sutton, R. P. Liu, and I. B. Collings, "Modelling IEEE 802.11 DCF heterogeneous networks with Rayleigh fading and capture," *IEEE Transactions on Communications*, vol. 61, no. 8, pp. 3336–3348, 2013.

[26] R. Nelson, *Probability, Stochastic Processes and Queuing Theory: Mathematics of Computer Performance and Analysis, Ser*, Springer-Verlag, New York, NY, USA, 1995.

[27] L. Hu, "Performance Evaluation of IEEE 802.11p EDCA for Vehicular Safety Communication Using Semi-markov Process," *Research Square*, https://doi.org/10.21203/rs.3.rs-1923692/v1, 2022.